Use of negative stiffness in failure analysis of concrete beams

A. Salam Al-Sabah Research Scientist, Debra F. Laefer Associate Professor*
Urban Modelling Group, School of Civil Engineering, University College Dublin, Ireland
*Corresponding author. E-mail address: debra.laefer@ucd.ie (D.F. Laefer).

Abstract

A new concrete analysis method is presented entitled continuous, incremental-only, tangential analysis (CITA). CITA employs piece-wise linear stress-strain curve and a tangent elasticity modulus to calculate stiffness including parts with negative values. Since indefinite structure stiffness matrices generally indicate instability, traditionally they have been avoided. However, since CITA analysis involves introducing damage in steps, the full range of concrete behaviour including the softening portion under tensile cracking can be addressed. Herein CITA is verified against numerical and experimental results for concrete beams, thereby showing faster solutions for non-linear problems than sequentially-linear analysis, while reducing self-imposed restrictions against negative stiffness.

Keywords: Concrete; Damage; Negative stiffness; Non-linear analysis; Sequentially linear analysis; Finite element

1. Introduction

Structural behaviour is rarely linear. Non-linearity stems from material behaviour and geometric effects [1] and [2]. Irrespective of the source of the non-linearity, non-linear structural analysis is more difficult and time consuming to perform than linear analysis. To avoid these difficulties, general engineering practice approximates non-linear behaviour using linearized behaviour. However, when a non-linear structure is analysed as a linear one, certain approximations related to the material and geometric properties must be made. These approximations are made by linearizing the non-linear properties, and results are only approximate. Notably, under careful linearization to satisfy certain design criteria, results can be used to produce safe designs.

An example is the linear analysis of reinforced concrete structures under ultimate loads. This first step is then followed by a second, in which the design of all critical components of the structure is done using local, nonlinear models. In such a two-step procedure, the component design is made using design material parameters, conservative models, or both, in order to ensure the intended reliability level [3]. Historically approximate results have been accepted mainly due to the difficulties encountered in the non-linear analysis of such structures in a one-step procedure. The outcome is a safe, although probably overdesigned, structure.

The topic of non-linear structural and stress analysis has undergone continuous progress during the last half century. To date, most methods have been used in conjunction with matrix structural analysis methods such as stiffness, finite element, and more recently, meshfree methods. While computer speed and storage capacity has aided this line of research, the main driver has been the need to develop better methods of modelling non-linear behaviour with

respect to efficiency, accuracy and solution robustness. Initial methods developed for the non-linear analysis of structures were the incremental tangent method, the iterative tangent method, and the incremental-iterative tangent method [1] and [2]. These methods were able to predict the behaviour of non-linear structures to the point where the tangent stiffness became zero (referred to as the limit point) [1].

For the analysis to move beyond limit points and other critical points, such as turning points, improvements to the basic incremental-iterative tangent analysis were made, mainly in the form of load control methods, displacement control methods, line search methods, and arc-length methods [1] and [2]. These solution methods are currently used in most finite element analysis packages such as ANSYS [4], ABAQUS [5] and ATENA [6]. However, difficulties are still encountered at bifurcation points [7] and in problems with significant strain softening [8] and [9]. Snap-through and snap-back responses have also been observed in reinforced concrete modeling due to cracking accompanied by spurious unloading caused by the arc-length procedure [1].

Conversely, non-linear solution methods have required the specification of many control parameters, which depended upon user experience. For highly non-linear problems, the incremental-iterative solution requires many small increments, each followed by a multitude of iterations, which entails a major time commitment to solve large problems. These difficulties stimulated the development of alternative methods [10] many of which rely on secant stiffness, which assures a non-negative stiffness matrix. While these approaches result in robust solutions, many analysis increments are required to cover the structural behaviour along the full load path.

A successful version of this type of approach is the sequentially linear analysis (SLA) method proposed by Rots [11] as a simplified non-linear finite element analysis for concrete during tensile cracking. SLA is based on re-analysing the structure at each increment from an unloaded state. The method addresses material softening behaviour by idealising the descending part of the stress-strain curve as a saw-tooth diagram (refer to Fig. 1). After crack initiation, the material secant modulus reduces in steps following the saw-tooth diagram. The diagram is constructed such that the area under the diagram is related to the crack fracture energy. Modified saw-tooth stresses fluctuate around the base value within a specific band. For each tensile strength (f_{ti}), a larger value (f_{ti}^{+}) is used to represent the maximum fluctuation limit, and a smaller value (f_{ti}^{-}) is used to represent the minimum fluctuation limit. The resulting softening part can be generated as a series of secant lines, each with a progressively reduced tensile strength and slope (E_i, E_{i+1}, …) and with a progressively increased maximum strain. As a result, the strain energy release from a cracking element is made correctly. Improved accuracy can be obtained by specifying more “teeth” in the diagram. The analysis results are a reflection of the saw-tooth diagram, with local sharp fluctuations of the load-deflection curve corresponding to the individual teeth. This method has since been extended and successfully applied to the material non-linear analysis of concrete with mesh regularisation [12], reinforced concrete [13], masonry [14] and [15], and glass [14], among other materials. This method was also applied to structural members loaded under shear [16], non-proportional loading [17] and [18] and snap-back of extremely brittle structures, such as glass [19].

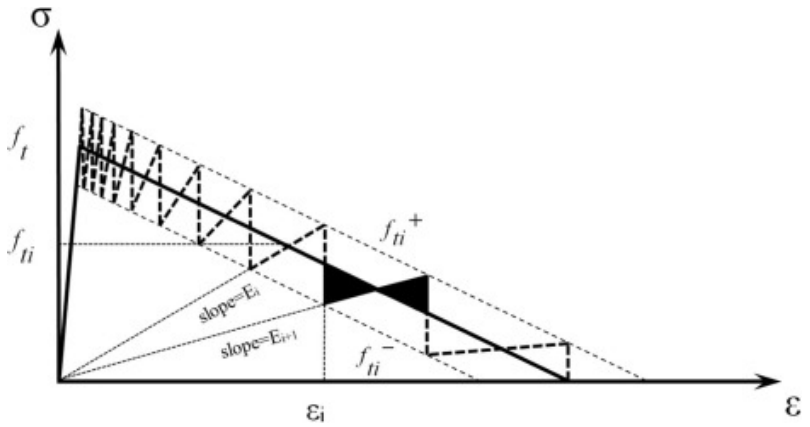

Fig. 1. Saw-tooth model.

Specifically, the method is "event by event" based. Hence, each analysis step requires resolving the stiffness equation. The result is a single event, such as damage to an undamaged element or more damage induced into an already damaged element. This event is shown as a point in the load-deflection curve. The secant stiffness of this element is reduced after the new damage. The structural stiffness equation is then modified to reflect this reduction and solved again. Thus, if there are 5 fully damaged elements, each represented by a stress-strain diagram of 10 teeth, then the stiffness equation must be solved 50 times. Depending upon the application, hundreds (and possibly thousands) of solution increments will be required (e.g. [15]). This is a major obstacle facing the use of the SLA method in solving structures having a large number of degrees of freedom and/or load steps [20]. The research presented herein was motivated by the difficulties encountered in solving the highly non-linear problem of concrete cracking in tension and provides an alternative to currently available tangent and secant methods in solving materially non-linear problems.

2. Background

The following paragraphs describe the background and details of the continuous, incremental-only tangential analysis (CITA) method. Major topics are the tangent stiffness matrix generation, matrix characterization and stiffness matrix (mathematical and structural).

2.1. Tangent stiffness matrix

The tangent stiffness is based on the tangent modulus of elasticity, E_t. For a non-linear stress-strain curve (cf. Fig. 2), the value of E_t can differ significantly at every point. For all points from the origin to (but excluding) point *A*, E_t is positive. At point *A*, E_t is zero. Beyond point *A*, E_t is negative.

In a geometrically linear analysis of simple 2D trusses, every element in the tangent member stiffness matrix is a function of E_t. Hence, the tangent stiffness matrices resulting from different values of E_t reflect the values and signs in their final characteristics. For positive values of E_t, the resulting tangent stiffness matrix is always positive definite and always negative definite for negative values of E_t. At point *A*, the tangent stiffness matrix is a zero matrix. On the other hand, the secant modulus of elasticity is always positive, hence always resulting in a

positive definite secant stiffness matrix. A similar argument can be presented for more complex continuum structures under more elaborate stress states.

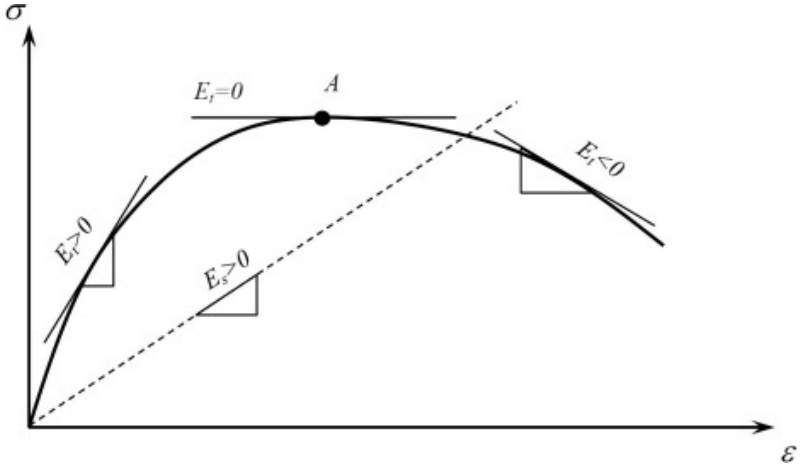

Fig. 2. Typical stress-strain curve.

2.2. Matrix characteristics

Stiffness-based structural analysis methods rely heavily on matrices, and the characteristics of stiffness matrices strongly influence the stiffness equation solution. The following two paragraphs briefly describe some of the relevant stiffness matrix characteristics from both a mathematical and structural point of view.

2.2.1. Mathematical characteristics

An eigenvalue, λ, of a square matrix, $\boldsymbol{K}$, is a value that satisfies the following relationship:

$$\text{for}: \ \boldsymbol{Kd} = \boldsymbol{f}, \ \boldsymbol{f} = \lambda \boldsymbol{d}, \ \text{or}: \qquad \boldsymbol{Kd} = \lambda \boldsymbol{d} \tag{1}$$

This means that the vectors $\boldsymbol{f}$ and $\boldsymbol{d}$ are parallel and that there exists a scalar eigenvalue, λ, which scales vector $\boldsymbol{d}$ to become equal to vector $\boldsymbol{f}$. These vectors are called the eigenvectors. A positive eigenvalue means that vectors $\boldsymbol{f}$ and $\boldsymbol{d}$ are in the same direction, while a negative eigenvalue means that the two vectors are in opposite directions.
Eigenvalues are used to categorise a square symmetric matrix as follows [21]:

- positive definite matrix when all its eigenvalues are larger than zero
- negative definite matrix when all its eigenvalues are smaller than zero
- indefinite matrix when some eigenvalues are larger than zero and others smaller than zero
- semi-definite matrix when some eigenvalues are equal to zero.

The following eigenvalue properties are also useful [21]:

- the determinant of a matrix equals the product of matrix eigenvalues;
- the eigenvalues of a matrix inverse equal the reciprocal of the matrix eigenvalues.

For a positive definite matrix with all positive eigenvalues, the determinant is positive. For indefinite matrices, the determinant sign can be positive or negative, depending upon the number of negative eigenvalues. For an evenly-numbered set of negative eigenvalues, the determinant is positive. Otherwise, it is negative. The application of the matrix characteristics described above on structural behaviour is described next.

2.2.2. Structural characteristics of stiffness matrix

Stiffness analysis is based on relating the displacements ***d*** to the loads ***f*** through a stiffness matrix ***K***, by Eq. (2):

$$\boldsymbol{K}\boldsymbol{d}=\boldsymbol{f} \tag{2}$$

The stiffness matrix of a structure is square and in most formulations symmetric. The structure's stiffness matrix results from assembling stiffness matrices of all the structure's elements followed by applying the essential boundary conditions. The determinant of an element stiffness matrix is zero. As the determinant of a square matrix equals the product of the matrix eigenvalues, the zero determinant implies that at least one eigenvalue is zero. The same is true for a structure stiffness matrix before imposing essential boundary conditions. A zero eigenvalue of a matrix means that the matrix is semi-definite. Such stiffness matrices result from unstable structures that have displacements ***d*** under no load ***f***, Eq. (1).

A typical linear stiffness analysis with normal boundary conditions leads to a positive definite structure stiffness matrix with all positive eigenvalues. The structure strain energy, *U*, will then be positive, Eq. (3).

$$U = 1/2\boldsymbol{d}^T\boldsymbol{K}\boldsymbol{d} = 1/2\boldsymbol{d}^T\lambda\boldsymbol{d} = 1/2\lambda\boldsymbol{d}^T\boldsymbol{d} > 0 \text{ for all } \boldsymbol{d}\neq 0 \tag{3}$$

Conversely, a negative eigenvalue results in negative strain energy, which signifies energy release.

3. CITA method

The CITA method attempts to control energy dissipation of a cracking concrete structure by limiting the damage level to a single event, such as concrete damage due to tension softening. From this perspective, there is a similarity with the SLA method [11] and [12]. However, rather than completely unloading and reloading the structure after each event using the current secant stiffness (as is done in SLA), CITA continues the analysis to the next event. As a result of this difference, the use of the tangent stiffness matrix (rather than the secant stiffness matrix in SLA) becomes necessary. The main advantage of this approach is its vastly improved efficiency, as will be demonstrated in Section 4.

3.1. CITA solution

In CITA, an incremental-only solution is adopted. When compared with usual incremental-iterative methods, the benefits of CITA are efficiency based, as there is no need to re-distribute

the internal stresses after each increment, thus, reducing analysis time. This scheme is possible in the current analysis, as long as the stress-strain curve is piece-wise linear. The general form of the stress-strain curve for concrete in tension used to demonstrate the formulation of CITA is shown in Fig. 3. Notably, a similar piece-wise linear curve was used by Graça-E-Costa et al. [9] in their study of a non-iterative approach for the modelling of quasi-brittle materials.

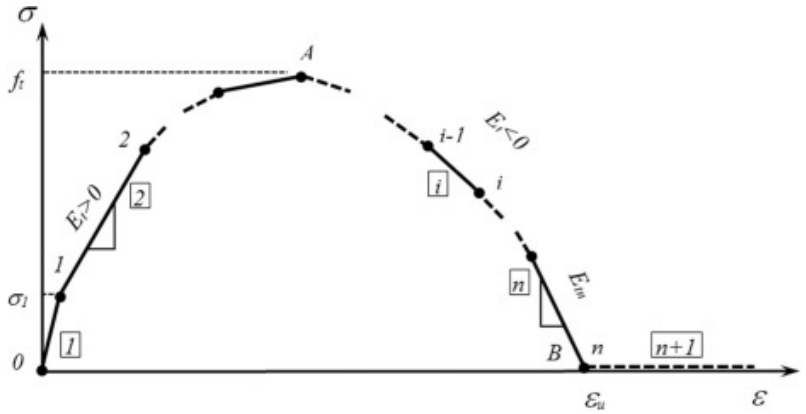

Fig. 3. Multi-linear concrete tension stress-strain damage model.

The model in Fig. 3 is made from (n + 1) straight lines. The first line has a positive slope representing the initial positive tangent modulus of elasticity, $E_t > 0$. Point *A* corresponds to the tensile strength; f_t. Lines beyond point A represent the descending part, which have negative slopes, hence negative tangent modulus of elasticity. Point *B* corresponds to the ultimate strain, ε_u, while the last part is line (n + 1) extending along the x-axis. This general model will be used in the current analysis. Furthermore, the adopted stress-strain curve of concrete in tension has no point with a zero slope, until complete failure occurs. As a result, the value of the tangent stiffness always differs from zero. A similar damage model can be adopted for concrete in compression.

The CITA method starts by assembling the structure's stiffness matrix based on the initial tangent modulus of elasticity. The essential boundary conditions are then introduced. The resulting stiffness matrix is positive definite. As damage is progressively introduced, new elements will have negative moduli of elasticity following the descending part of the stress-strain curve. These damaged elements will change the structure tangent stiffness matrix to indefinite, as damage progresses.

The current analysis using CITA is for proportional loading only. The solution is static and based on small displacements. Damage is assumed to develop due to tension only.

The analysis is conducted according to the following steps:

a) Element stiffness matrices are calculated based on current tangent modulus of elasticity.
b) A structure global tangent stiffness matrix, ***K***, is assembled.
c) Essential boundary conditions are imposed.
d) A load vector, ***f***, is calculated based on unit loads.
e) Total result matrices are initialized:

$$\text{total deflection } \boldsymbol{d_t} = \boldsymbol{0} \tag{4}$$

$$\text{total element forces (and stresses) } \boldsymbol{f_{m,t}} = \boldsymbol{0} \tag{5}$$

f) A solution increment is initialized: *inc* = 0
g) A solution increment is increased by one: *inc* = *inc* + 1
h) The stiffness equation is solved:

$$\boldsymbol{K d = f \rightarrow d = K^{-1} f} \tag{6}$$

i) Element forces (and stresses) are calculated, $\boldsymbol{f_m}$.
j) The concrete element, e_i, closest to the tension damage is identified.
k) The load factor, L_{fe}, required to scale element e_i forces of the current increment to cause damage in element e_i is calculated. The increment load factor, L_f, is calculated from L_{fe} as presented in Section 3.4.
l) Incremental results are scaled by the load factor:

$$\boldsymbol{d_{inc} = L_f d,\ f_{m,inc} = L_f f_m} \tag{7}$$

m) Incremental results are added to total results:

$$\boldsymbol{d_t = d_t + d_{inc}} \tag{8}$$

$$\boldsymbol{f_{m,t} = f_{m,t} + f_{m,inc}} \tag{9}$$

n) The modulus of elasticity of element e_i is revised to its new value.
o) The tangent stiffness matrix of element e_i is calculated based on the revised modulus of elasticity.
p) The global tangent stiffness matrix is revised based on the revised stiffness of element e_i.
q) Steps (g) to (p) are repeated, until the stopping criteria are satisfied.

While many of above solution steps are typical for incremental solutions, the CITA method differs from other incremental solutions in three major aspects: (1) how the stiffness equation is solved (step h), as discussed in Section 3.2; (2) use of the negative tangent modulus of elasticity (step n), as discussed in Section 3.3; and (3) calculation of the load factor (step k), as discussed in Section 3.4. A description of concrete cracking used in CITA is presented in Section 3.5.

3.2. Factorizing matrices

The stiffness Eq. (2) solution involves calculating the structure stiffness matrix inverse. This operation requires dividing the adjoint, $Adj\boldsymbol{K}$, by the determinant, $|\boldsymbol{K}|$, of the structure stiffness matrix.

$$\boldsymbol{K^{-1} f} = Adj\boldsymbol{K} / |\boldsymbol{K}| \boldsymbol{f = d} \tag{10}$$

The matrix $\boldsymbol{K}$ is invertible, if and only if, its determinant does not equal zero $|\boldsymbol{K}| \neq 0$ [21]. Hence, there is the potential to calculate the inverse of positive definite, negative definite, and indefinite matrices. However, calculating the inverse of semi-definite matrices is not possible. Based on that, and contrary to the belief of many engineers, a stiffness matrix with a negative stiffness can be solved. The results might not be intuitively imagined easily, particularly given the long history of negative opinions in this regard, but such results can be correct, as will be demonstrated by the examples presented in Section 4.

Calculating the inverse of large matrices is not the most numerically efficient method to solve Eq. (2). Instead, the Cholesky decomposition is commonly adopted [21]. However, this method in its basic form can only decompose a positive definite matrix due to the need to calculate diagonal square roots. To factorise an indefinite matrix efficiently, methods such as the Bunch and Kaufman method [22] or Aasen's method [23] need to be used. These are generally based on an $\boldsymbol{LDL}^T$ decomposition [24] and can be used without significant efficiency reduction as compared to a Cholesky decomposition.

3.3. Negative tangent modulus of elasticity

As discussed in Section 2.2.2, the formulation of a typical stiffness matrix leads to positive definite structure stiffness matrices and positive strain energy.

A typical axial member of positive stiffness can be imagined as a spring that when pulled and extended in length tends to produce a force that resists the movement. On the other hand, an axial member with a negative tangent stiffness tends to produce a force that assists the movement. Therefore, a member with a negative tangent stiffness is unstable when acting alone. This is the reason why upon detecting a negative stiffness along the stiffness matrix's diagonal during the assembly or factorization stages, many stiffness and finite element packages produce a warning or stop altogether.

A negative tangent stiffness is encountered in practice in different forms and can be used favourably in some applications. The tactile behaviour of some high-end calculator keypads is one such example. This behaviour is based on the snap-through buckling of arch- or dome-shaped, thin metal plates that guarantee a good circuit contact [25]. This snap-through buckling exhibits negative stiffness characteristics. On a larger scale, negative stiffness devices (NSD) can be used to reduce seismic forces, drifts, and accelerations above the level at which they are installed [26].

Although unstable by themselves, members with a negative tangent stiffness can be part of a larger system where their instability can be contained by other parts of the system. An example is a reinforced concrete beam developing tension cracks due to a bending moment. The concrete cracking process can be modelled as a continuous softening induced by damage. The initially positive tangent stiffness of uncracked concrete will ultimately reduce to zero (and with no strength), in the case of fully tension-damaged concrete. A negative stiffness must be involved in order to reduce the positive tangent stiffness to zero stiffness and strength, after complete damage occurs. A reinforced concrete beam, as a whole system, will lose some of its stiffness but remain stable, if the reinforcement can restrain the crack propagation.

In CITA, stiffness matrices with some negative eigenvalues (i.e. indefinite matrices) are accepted. The resulting stiffness equation can still be solved as described in Section 3.2. The

unstable structural behaviour resulting from the negative strain energy (Section 2.2.2) usually associated is controlled by limiting damage progress to a single incident, as will be described in the next section.

3.4. CITA load factor calculation

Load is applied in increments. The result of each analysis increment is the occurrence of damage in a previously undamaged element or the generation of more damage to an already damaged element. The load factor can be positive or negative depending on the damage level of the whole structure. The principle of calculating the load factor is to find the smallest change in external incremental load that produces the next damage occurrence. Determination of the load factor value is based on the piece-wise linear stress-strain diagram, Fig. 3. For an element e , stressed to a total stress of $\boldsymbol{\sigma_e}$ (resulting from previous increments) and an incremental stress of $\Delta\boldsymbol{\sigma_e}$ (resulting from the current increment due to a unit load), the load factor is calculated as follows:

a) For an undamaged element:

$$\boldsymbol{L_{fe}} = \frac{\boldsymbol{\sigma_1} - \boldsymbol{\sigma_e}}{\Delta\boldsymbol{\sigma_e}} \tag{11}$$

where $\boldsymbol{\sigma_1}$ corresponds to the stress at point *1* in the stress-strain diagram, Fig. 3.

b) For an already damaged element with stress level within line *i* of the stress-strain diagram:

$$\boldsymbol{L_{fe}} = \frac{\boldsymbol{\sigma_i} - \boldsymbol{\sigma_e}}{\Delta\boldsymbol{\sigma_e}} \tag{12}$$

where $\boldsymbol{\sigma_i}$ corresponds to the stress at point *i* in the stress-strain diagram, Fig. 3.

c) For elements that are completely damaged with strain at point *B* or more, where the tangent modulus of elasticity is zero, a small negative value of $-E_{tn}/100{,}000$ is used instead of zero to keep the stiffness matrix non-singular.

The scalar element load factor L_{fe} is calculated from the element load factor vector $\boldsymbol{L_{fe}}$ as the value that has the minimum absolute value of $\boldsymbol{L_{fe}}$. Once the load factors resulting from all elements are found, the load factor (L_f) at the current increment is the element load factor, L_{fe}, which has the minimum absolute value.

The value of (L_{fe}) as calculated from Eqs. (11) and (12) can be positive or negative, depending on the stress state of the element and the new incremental stress. Referring to the load factor's general equation for an element, Eq. (12), the term $\boldsymbol{\sigma_i}$ is always positive (but can also be zero – point B in Fig. 3). For a member with a total tensile stress at the current load increment, $\boldsymbol{\sigma_e}$ is also positive. The term ($\boldsymbol{\sigma_i}$-$\boldsymbol{\sigma_e}$) is positive when the element stress state is still within the ascending part of the stress-strain diagram with a positive tangent modulus of elasticity. Otherwise, the term is negative. Finally, the term $\Delta\boldsymbol{\sigma_e}$ is positive for all elements at the start of analysis. At later analysis stages when more damage is introduced into the elements, $\Delta\boldsymbol{\sigma_e}$ can be negative (e.g. for an element with tensile stress beyond point A in Fig. 3). Based on the above discussion, the element load factor L_{fe} can be positive or negative. The

load vector ***f*** used in the analysis is based on a unit vector and is applied to all load increments. Hence, the displacements calculated from Eq. (6) depend on the stiffness matrix state only. The CITA method is based on a continuous increase in the damage level, as the solution progresses. Stiffness will reduce accordingly. Deflection of a specific node called the control node is used as an indicator of such behaviour. At the early stages of damage, only a few damaged elements will have a negative tangent stiffness, and the structure tangent stiffness matrix will still be positive definite. The slope of the load-deflection curve of the control point is positive, and the deflection of that point is in the same direction as the unit load. At such loading stages, the load factor will generally be positive. As the damage level increases, more elements will be in the tension softening stage of behaviour. These elements will have some stiffness components based on negative tangent stiffness. Introducing such element stiffness matrices will slowly change the structure stiffness matrix to become indefinite. As a result, displacements can be in the opposite direction to that of the applied loads. Under such conditions, a negative load factor can be obtained.

Within a certain solution cycle, the structure has linear behaviour within the assumed piece-wise linear stress-strain curve. The linear behaviour extends up to the point on the stress-strain curve where the next linear piece starts. Load factor calculations were based on capturing this point. At the next cycle, the stiffness matrix of the element affected by the slope change is based on the changed value. Hence, energy equilibrium is maintained, and there are no unbalanced forces or local unloading that require redistribution.

3.5. Cracking

A major cause of the non-linear behaviour of concrete is tension cracking. The sudden release of strain energy during cracking is the reason behind the numerical difficulties encountered in modelling this phenomenon. Cracking can be modelled discretely as an actual separation of materials across a crack [27] and [28]. Then crack width, crack tip stress, and crack direction can be determined. The results obtained from discrete methods can be quite accurate, particularly when a fine mesh is used at the crack tip in a finite element method. However, this accuracy comes with the heavy penalty of needing to update the numerical model topology as each crack propagates through the media. Due to the cost of this penalty, this method is mainly used for particularly detailed analysis of important structures.
A numerically more economical alternative is the smeared crack method, first introduced in 1968 by Rashid [29]. The efficiency of this method as compared with the discrete cracking method is the result of maintaining the same geometric model. Actual cracks are approximated by idealised smeared cracks that are assumed to be distributed over the finite element width. The constitutive properties are revised based on the calculated crack direction. Due to the approximate nature of the smeared cracking method, some of the behaviour details are inevitably lost. For more details of these two methods see Borst et al. [30].

Other, more recent methods of modelling discontinuities such as the extended FEM can also be used to model cracking. In this method, special enriching functions are added to the finite element approximation using the framework of partition of unity [31]. Notably, there is no need to modify the model topology with the crack propagation, as strong discontinuities can

be modelled. However, the enrichment requires substantial numeric calculations that can slow the analysis.

Other concrete constitutive models that allow for cracking (such as the nonlocal method [32], plasticity models [33] and plasticity damage models [34]) are available. These methods can handle more complex stress states of concrete at the cost of more computations. Regardless of the method used, the solution has to handle negative tangent stiffness, an issue CITA attempts to address.

The CITA method is not limited to the use of a particular crack modelling method, as its aim is to model the non-linear behaviour of concrete. In the present research, the method adapted to model cracking is the smeared method. In applying this method for crack analysis of concrete, it was previously observed [35], [36] and [37] that finite element results depend on element size. To maintain mesh objectivity and independence, Bazant and Cedolin [35] and [36] proposed the concept of crack band width, *h*, to normalize the stress-strain curve with the aim of maintaining constant fracture energy. Following that concept, Rots and Invernizzi [12] proposed using Eq. (13) to regularize the ultimate strain, $\in_u$, by relating it to the fracture energy, G_f, tensile strength, f_t, and crack band width, h.

$$\epsilon_u = 2\left(\frac{G_f}{h}\right)/f_t \tag{13}$$

The resulting value of $\in_u$ is used to construct the stress-strain curve of concrete in tension (refer to Fig. 5).

4. Numerical validation study

The CITA method, as described above, was implemented in a new software code using MATLAB. The general structure of the code is as described in steps a-q in Section 3.1. All examples were solved on a computer with an Intel Xeon E31225 CPU running at 3.1 GHz with 8 GB RAM and a 64 bit operating system.

4.1. Example 1

To test the applicability of the proposed method, a previously studied beam was modelled, Fig. 4. It was used by DeJong et al. [17] to demonstrate the applicability of SLA to non-proportional loading. The beam is a hypothetical concrete beam that was solved by DeJong et al. [17] using an incremental-iterative analysis. The symmetric concrete beam was 500 mm long, with a 450 mm span. The cross-section was 100 mm × 100 mm. Load was applied at the third points of the free 450 mm span. The beam was assumed to have the stress-strain diagram in tension shown in Fig. 5 with an initial modulus of elasticity, E_{t1}, of 32 GPa, and an initial tensile strength, f_t, of 3 MPa. This simple model was suggested and used by many researchers to model concrete damage in tension [10], [13] and [37]. The fracture energy was assumed to be 0.06 N mm/mm^2, and the beam was assumed to crack only within a 20 mm wide zone at its mid-span [17]. No cracks were assumed to develop in concrete due to compression.

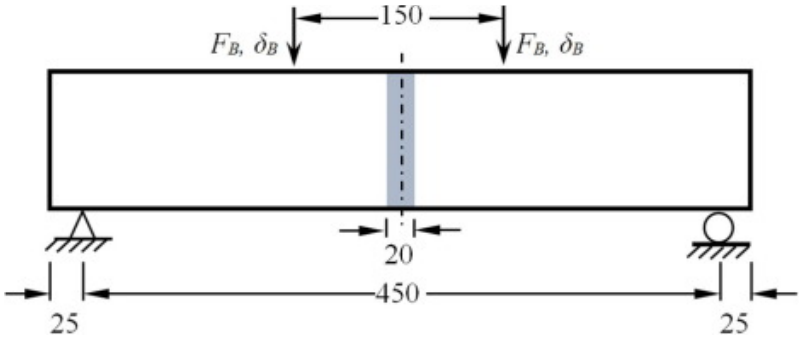

Fig. 4. Geometry, loading and supports of studied concrete beam.

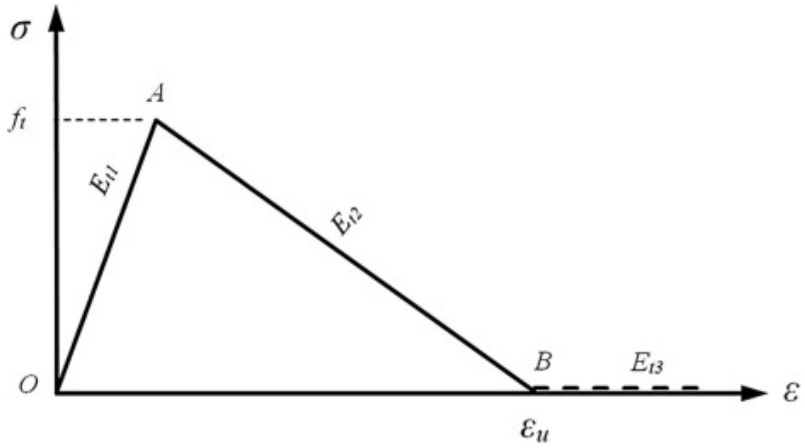

Fig. 5. Stress-strain diagram for Example-1 as used by DeJong et al. [13].

The maximum, constant, bending moment was generated within the beam's middle third. The beam was previously studied numerically using different methods including non-linear finite element analysis and SLA [17]. The problem was also solved by Graça-e-Costa et al. [38] using a pair of incremental-only methods that combined tangents and secant solutions. The crack band width, *h*, used in these analyses was constant and had a value of 20 mm, the same value used by DeJong et al. [17].

The CITA method can be applied to any element type. The most obvious type to be used in modelling beams is 2-D finite elements. However, the model requires many such elements to achieve a reasonable accuracy. To demonstrate the CITA method in a simple way that can be easily followed, a simple 1-D frame element is introduced below. This is then followed by an implementation using 2-D finite elements.

4.1.1. CITA solution using 1-D frame elements

The concrete beam shown in Fig. 4 is modelled using 1-D frame elements. The middle 20 mm of the beam was assumed to be the cracking zone as used in the reference solution by DeJong et al. [17]. This portion was modelled by 1-D frame elements with the stress-strain diagram shown in Fig. 5. These elements were called the cracking elements. All other elements were assumed to maintain their initial linear elastic properties throughout the analysis. Three models, with an increasing number of cracking elements, were used to study the beam (Fig. 6). These models were named B6, B16, and B32 for the models containing 6, 16, and 32 cracking

elements (respectively) in the middle 20 mm of the beam. These elements have section properties that depend upon their spacing. Their moment of inertia was reduced by a factor of 1000 to maintain mainly axial behaviour in the cracking elements, while keeping the structure stable. The beam was modelled with horizontal elements running at mid-depth of the concrete beam and with the concrete beam section properties. Two vertical elements at the model ends had lengths of half the cross-section's depth. Supports were provided at the end of these two members. The section properties of these elements were the same as those used for the main beam. In addition, two vertical sets of frame elements (one on each side of each cracking element) were used to link the cracking elements to the main beam elements. The cross-sectional area of these elements was the same as that of the main beam elements, while their moment of inertia was 2.5×10^6 mm^4. This value was used to bring the results from the current 1-D analysis as close as possible to those resulting from the 2-D analysis. The models were loaded by a pair of downward base loads at the beam's third points, each of 1 kN. The adopted material properties in this analysis were the same as those used by DeJong et al. [17] and Graça-E-Costa et al. [38]. In all three models, the control node was the same as the loaded node. The analysis was continued, until the stopping criterion of the control node deflection exceeding 0.3 mm was satisfied.

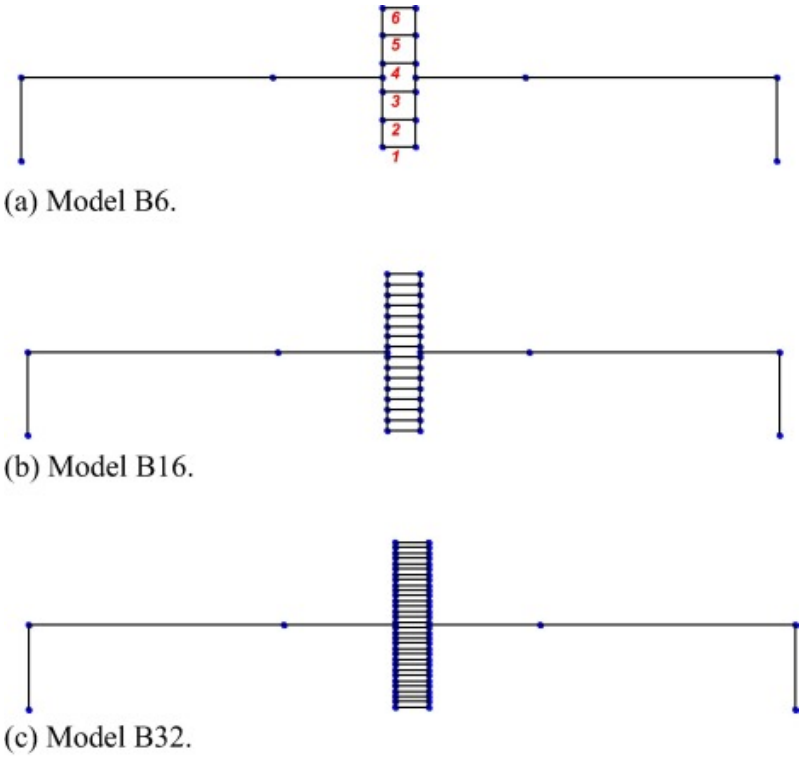

Fig. 6. Idealised beam models.

The detailed results from beam B6 are presented for the first 6 increments in Table 1, Table 2, Table 3, Table 4, Table 5 and Table 6 to demonstrate the CITA solution. The tables show the cracking elements (1–6), the tangent modulus of elasticity, and the total stress at the start of each solution increment, the incremental stress due to the applied base load, and the calculated increment load factor for each element based on Eqs. (11) and (12). The bottom two

rows show the incremental and total load factors, as well as the incremental and total deflections of the control node.

Table 1.
Results from B6 model, increment 1.

Increment 1, ***K*** is positive definite

Element no.	E_t (MPa)	σ_e (MPa)	$\Delta\sigma_e$ (MPa)	L_{fe}
1	32,000	0	0.649	**4.625**
2	32,000	0	0.607	4.939
3	32,000	0	0.335	8.963
4	32,000	0	−0.335	−8.963
5	32,000	0	−0.607	−4.939
6	32,000	0	−0.649	−4.625
ΔL_f	4.625		$L_{f,\,\text{total}}$	4.625
$\Delta\delta$ (mm)	−0.012		δ_{total} (mm)	−0.057

Table 2.
Results from B6 model, increment 2.

Increment 2, ***K*** is positive definite

Element no.	E (MPa)	σ_e (MPa)	$\Delta\sigma_e$ (MPa)	L_{fe}
1	−1571	3.000	−0.102	29.393
2	32,000	2.809	1.363	**0.140**
3	32,000	1.548	0.609	2.383
4	32,000	−1.548	−0.326	−13.968
5	32,000	−2.809	−0.721	−8.060
6	32,000	−3.000	−0.824	−7.278
ΔL_f	0.140		$L_{f,\,\text{total}}$	4.765
$\Delta\delta$ (mm)	−0.013		δ_{total} (mm)	−0.059

Table 3.
Results from B6 model, increment 3.

Increment 3, ***K*** is positive definite

Element no.	E (MPa)	σ_e (MPa)	$\Delta\sigma_e$ (MPa)	L_{fe}
1	−1571	2.986	−0.435	6.867
2	−1571	3.000	−0.285	10.511
3	32,000	1.633	2.920	**0.468**
4	32,000	−1.594	0.441	10.426
5	32,000	−2.910	−0.925	−6.386
6	32,000	−3.115	−1.715	−3.566
ΔL_f	0.468		$L_{f,\,\text{total}}$	5.233
$\Delta\delta$ (mm)	−0.017		δ_{total} (mm)	−0.067

Table 4.
Results from B6 model, increment 4.

Increment 4, ***K*** is indefinite

Element no.	E (MPa)	σ_e (MPa)	$\Delta\sigma_e$ (MPa)	L_{fe}
1	−1571	2.782	10.743	−0.259
2	−1571	2.866	7.610	−0.377
3	−1571	3.000	4.659	−0.644
4	32,000	−1.387	−43.815	**−0.100**
5	32,000	−3.343	−5.093	−1.245
6	32,000	−3.918	25.897	0.267
ΔL_f	−0.100		$L_{f,\,\text{total}}$	5.133
Δδ (mm)	0.134		δ_{total} (mm)	−0.080

Table 5.
Results from B6 model, increment 5.

Increment 5, ***K*** is indefinite

Element No.	E (MPa)	σ_e (MPa)	$\Delta\sigma_e$ (MPa)	L_{fe}
1	−1571	1.706	0.762	**−2.239**
2	−1571	2.104	0.585	−3.598
3	−1571	2.533	0.421	−6.019
4	−1571	3.000	0.280	−10.728
5	32,000	−2.833	−2.571	−2.269
6	32,000	−6.511	0.524	18.157
ΔL_f	−2.239		$L_{f,\,\text{total}}$	2.894
Δδ (mm)	−0.002		δ_{total} (mm)	−0.075

Table 6.
Results from B6 model, increment 6.

Increment 6, ***K*** is indefinite

Element no.	E (MPa)	σ_e (MPa)	$\Delta\sigma_e$ (MPa)	L_{fe}
1	−0.32	0.000	0.000	−4.7E+16
2	−1571	0.794	1.605	−0.495
3	−1571	1.591	1.157	−1.375
4	−1571	2.374	0.726	−3.269
5	32,000	2.925	−5.942	**−0.013**
6	32,000	−7.684	2.454	4.354
ΔL_f	−0.013		$L_{f,\,\text{total}}$	2.881
Δδ (mm)	0.014		δ_{total} (mm)	−0.075

Table 1 shows the results of increment 1. The structure had a positive definite stiffness matrix. Element 1, at the bottom of the cracking beam zone, was the most highly stressed element in tension. The increment load factor of 4.625 was calculated on the basis of stressing this element to its ultimate strength.

Increment 2 started with cracked element 1 having a negative tangent modulus of elasticity. However, the structure stiffness matrix was still positive definite. The next element to crack was element 2 with an incremental load factor of 0.140. The incremental deflection of the control node (before the introduction of the incremental load factor) was slightly larger than that resulting from increment 1, thereby indicating a beam stiffness reduction after the cracking of element 1 at the end of increment 1.

The next element to crack was element 3, increment 3. The structure continued to lose stiffness due to the reduced stiffness of cracked elements 1 and 2. However, the structure stiffness matrix was still positive definite.

Increment 4 started with 3 cracked elements out of the 6 total. The structure's stiffness matrix was indefinite at this stage. Incremental deflection of the control node was 0.134 mm in the direction opposite to the load direction. In addition, the deflection's absolute value was much larger than those from previous increments. For the first time, the increment load factor was negative. The critical element was element 4, which was in compression at the start of the increment. The meaning of the negative load factor at this increment is that the structure was losing its load-carrying capacity as the total load was reducing. This behaviour can be observed from the load-deflection curve of the control node as shown in Fig. 7. Referring to Eq. (12), the term σ_i was 3 MPa, σ_e was −1.387 MPa, and $\Delta\sigma_e$ was −43.815 MPa. These values will result in the term $(\sigma_i - \sigma_e)$ to be 4.387 MPa. The element load factor will have the negative value of −0.100.

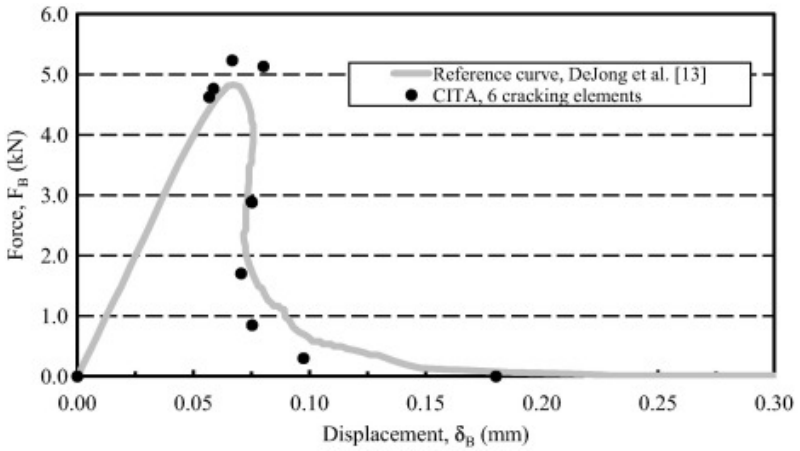

Fig. 7. Load-deflection curve of control node, B, resulting from model B6 analysis.

A new limit was reached at the end of increment 5, as element 1 was the first element to fail completely when reaching point B in the tension stress-strain curve (see Fig. 3 and Fig. 5). The structure stiffness matrix was indefinite. The increment load factor was negative with a large absolute value associated with a relatively small incremental deflection of the control node. This signifies a sharp, nearly vertical drop in the load-deflection curve of the control node, as shown in Fig. 7. The structure was quickly losing its load-carrying capacity at this stage. Increment 6 started with the completely failed element 1 having a very small tangent modulus of elasticity (instead of zero). This was done to keep the structure stiffness matrix from being singular. Another possible approach would be to completely remove this element from the

analysis. However, this would require re-defining the geometry, which can complicate the analysis. Both the load factor and incremental deflection of the control node were small. The associated point on the load-deflection curve is barely distinguishable from the previous point.

The analysis continued for 10 increments until the control node specific deflection limit was exceeded. The resulting load-deflection curve is shown in Fig. 7. In spite of the model simplicity, it managed to capture the beam behaviour as compared to the reference curve. The reference curve refers to the results obtained by DeJong et al. [17] using an incremental-iterative analysis. The analysis was repeated with 16 cracking elements and again with 32. The load-deflection curves of the control node are shown in Fig. 8. These results indicate a progressive improvement as the total number of cracking elements was increased. Peak load was found to be 5.2 kN, 5.3 kN, and 5.3 kN from the analysis of models B6, B16, and B32, respectively.

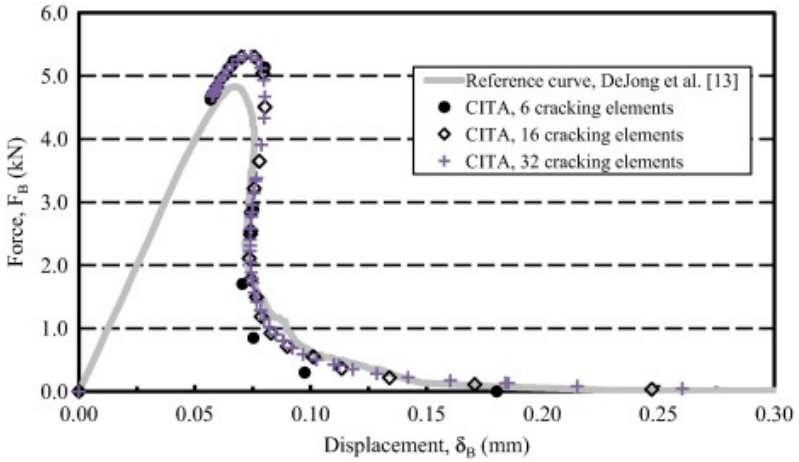

Fig. 8. CITA load-deflection results of B6, B16, and B32.

These results compared well with the reference value of 4.8 kN obtained from the NLFEM. The CITA load-deflection curves managed to capture reasonably well the beam behaviour as obtained from NLFEM. As more cracking elements were used, the CITA results were closer to the reference response. However, the CITA results were obtained from a much simpler structural model using 1-D elements rather than the 2-D elements with four integration points used in the reference model.

4.1.2. CITA solution using 2-D, plane stress elements

To demonstrate the applicability of the CITA method when used with typical finite element analysis, the method was implemented in a new code. Plane stress, quadrilateral, isoparametric elements with 4 nodes per element were used. The model is shown in Fig. 9.

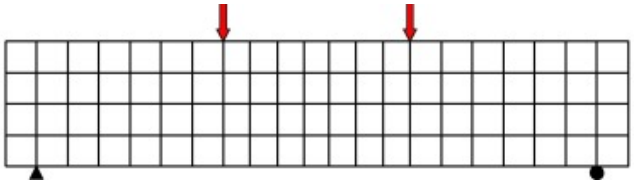

Fig. 9. Finite element model.

Load was applied at the same nodes as in Fig. 4, and the material properties were as earlier. All elements had a 2 × 2 Gaussian integration scheme, except the central 4 elements at mid-span. Those had 1 × 4 integration points. Only those 4 elements were considered to be cracking elements with tension stress-strain behaviour as shown in Fig. 5. All other elements maintained their initial linear elastic properties throughout the analysis. The model is similar to the model used to produce the reference results [17]. The model symmetry and set-up resulted in vertical cracks at the central elements only. Isotropic material properties were used to represent the concrete. However, orthotropic material properties were used to represent cracking concrete at mid-span. That was necessitated by the fact that all cracks were in one direction only. The tangent modulus of elasticity in the horizontal x-direction, E_{tx}, was changed through the analysis based on Fig. 3 and Fig. 5. The tangent modulus of elasticity in the vertical y-direction, E_{ty}, was kept constant and equal to the initial tangent value. To keep the stiffness matrix symmetric, Poisson's ratios v_{xy} and v_{yx} were related such that E_{tx}/v_{xy} was made equal to E_{tx}/v_{yx}.
The load-deflection results of point B (Fig. 4) are shown in Fig. 10. The CITA was completed in 30 steps (the last result is not shown as the deflection exceeded 0.3 mm). As expected, the results obtained from the 2-D finite element analysis are closer to the reference results than the previous results obtained from the 1-D element model.

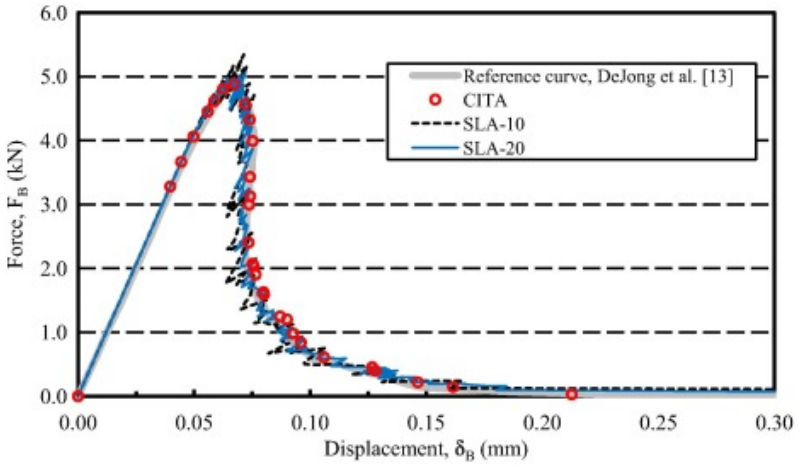

Fig. 10. Load-deflection curves from SLA and CITA methods.

An analysis using SLA was also conducted to compare its results with those obtained from CITA. The analysis was based on a saw-tooth diagram similar to that shown in Fig. 1 with 10 and 20 teeth. The analysis was completed in 135 and 284 steps using the 10 and 20 teeth models, respectively. The number of steps and solution time comparison between the SLA and CITA are shown in Table 7.

Table 7.
CITA and SLA relative solution time comparison.

Item	CITA	SLA	
		10 teeth	20 teeth
No. of solution steps	30	135	284
Run time (s)	3.75	16.87	35.50
Relative solution time	1	4.50	9.47

Both SLA and CITA results are close to the reference results and to each other as shown in Fig. 10. The CITA results, however, are smoother than the SLA results, showing consistent proximity to the reference curve. In addition, as each analysis step took nearly the same time to run in both methods, the CITA method completed the analysis in less than a quarter of the time required for the SLA with 10 teeth (Table 7). If smoother results are required from SLA analysis, more teeth would be required. The SLA analysis was repeated using 20 teeth (Fig. 10). The results were improved, but 284 analyses were required, thereby more than doubling the previous SLA analysis time. This makes the CITA time nearly 9.5 faster than the SLA analysis time, Table 7. This advantage of CITA, however, will reduce as the shape of the stress-strain curve becomes more complex. The current CITA method was based on the piece-wise linear stress-strain curve shown in Fig. 5, which was made from three lines.

4.2. Example 2

To test CITA results against experimental results, a beam tested by Petersson [39] was used. This beam was selected due to the fact that the beam experiment was repeated several times and that the concrete material parameters have been carefully studied and specified. The concrete beam was 2000 mm in span, 200 mm deep and 50 mm thick. It had a 100 mm notch at mid-span. The notch width was taken as 20 mm. The beam was loaded at mid-span. The initial modulus of elasticity was 30 GPa, the tensile strength was 3.33 MPa, Poisson's ratio was 0.2, and the fracture energy was 0.124 N mm/mm^2. The beam was assumed to crack only within a 20 mm wide zone at its mid-span. The finite element mesh used in the CITA analysis is shown in Fig. 11.

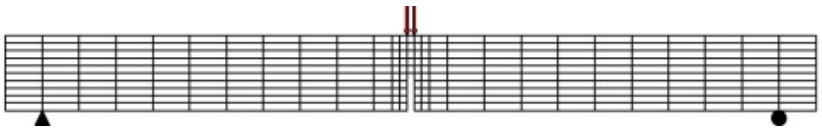

Fig. 11. Finite element model of experimental notched beam tested by Petersson [34]

The crack band width used in the analysis was 20 mm. All elements had a 2 × 2 Gaussian integration scheme, except the central 5 elements at mid-span, which had 1 × 4 integration points. After tension cracking, orthotropic material properties similar to those used in Example 1 were used. Concrete was assumed to be linear elastic in compression.

The stress-strain curve for concrete in tension used in this example is shown in Fig. 12. This model is based on the model adopted by the International Federation for Structural Concrete [40].

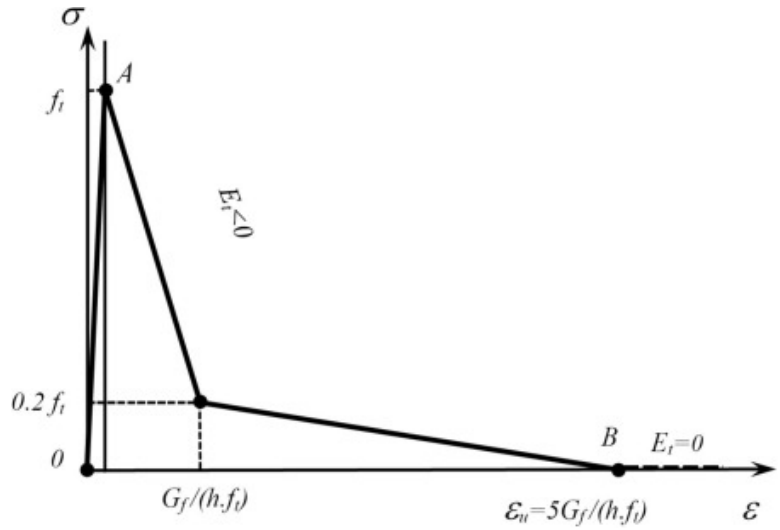

Fig. 12. Concrete tension stress-strain model.

The CITA load-deflection results of the loaded points are shown in Fig. 13. These results were based on a value of Gf = 0.124 N mm/mm^2. The experimental results are shown for the following two values: Gf = 0.115 N mm/mm^2 and Gf = 0.137 N mm/mm^2. CITA accurately followed the behaviour of the beam along its full load history using an intermediate loading value with respect the two experimental ones.

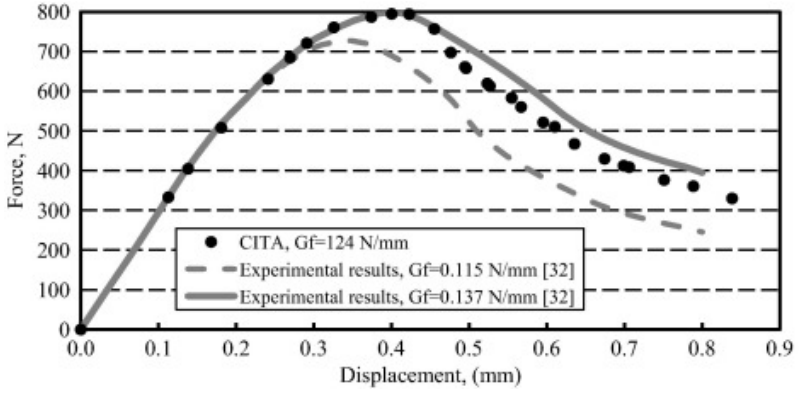

Fig. 13. Load-deflection curves results of the Patersson experimental beam [34].

4.3. Discussion

Non-linear finite element analysis is the most obvious solution technique to solve non-linear structural analysis problems. When limit points are present, the incremental-iterative solution with arc-length control, or one of its variations, is usually used. However, structures with significant tension crack softening behaviour, such as concrete beams cracking in tension, are particularly challenging problems to solve. Small arc-lengths are required, which leads to long analysis times. Even then, many cracks will be generated at each solution step. As this problem behaviour is path-dependent, this broad crack generation can possibly lead to unrealistic results [10]. In response, SLA solves this issue by increasing damage by one event at a time.

However, this is achieved at the cost of extended analysis time. While there is some analysis time penalty involved in the process of increasing damage one step at a time, a significantly more substantial time penalty is, in fact, related to the use of the saw-tooth model. This model is necessary for the gradual release of strain energy and in keeping the stiffness matrices positive definite. This is achieved by using the secant, rather than the tangent, modulus of elasticity. To cause a complete failure in a tension element, SLA needs a number of analysis increments equal to the number of saw-teeth in the stress-strain curve. This number needs to be large enough to obtain relatively smooth behaviour and to release crack fracture energy. The CITA method is based on increasing structural damage one step at a time. In this respect, the proposed method bears similarity to the SLA method but differs significantly in how the stress-strain curve is used. While SLA uses the saw-tooth model, CITA uses a piece-wise linear stress-strain curve. The need for the SLA saw-tooth model results from the need to use the always positive secant modulus of elasticity. On the other hand, CITA accepts the existence and use of a negative tangent modulus of elasticity. This will usually lead to indefinite structure stiffness matrices at later stages of damage analysis. Such matrices are an indication of instability but they can still be factorized and used to continue the structural analysis. However, the analysis has to be controlled. The control method adopted in this research was to limit damage to one event at a time. The piece-wise linear stress-strain curve adopted in CITA leads to an incremental-only solution rather than the loading-unloading scheme of SLA. CITA also results in substantial reduction of analysis time, as damage is not controlled by the saw-tooth model and because fracture energy can be correctly and smoothly released.

CITA combines the best features of both the incremental-iterative, non-linear and SLA methods. The solved reference problem showed that even with a coarse model, CITA can predict the complex softening behaviour in a few steps and was able to produce smooth and accurate results. The efficiency advantage of CITA relative to SLA was illustrated in Example 1, where it was shown that CITA can be 4.5 and 9.47 times faster than SLA for a number of teeth of 10 and 20, respectively (as shown in Table 7). In addition, CITA does not suffer from the local sharp fluctuations of the load-deflection curve corresponding to the individual teeth as shown in Fig. 10. The CITA method managed to produce accurate results, even when a simple structural model was used. In solving Example 1, CITA proved able to accurately predict the full behaviour range, even when 6 cracking 1-D elements were used.

The CITA solution was stable, and no numerical difficulties were encountered. Use of 2-D elements produced better results as these were more accurate in representing the beam. CITA results were also close to the experimental test results as shown in Fig. 13 of Example 2, where CITA results were shown to be between the two extremes of test results.

One aspect of CITA that deserves further investigation is the possibility of encountering singularity during solution generation. As long as the modulus of elasticity is not zero, all diagonal stiffness coefficients are other than zero. This in and of itself does not necessarily guarantee that the global stiffness matrix is not singular. One can consider the possibility of a node connecting two elements of which one is damaged and the other undamaged. In such a case, there is a possibility that at one degree of freedom of that the node would have a positive diagonal value from the undamaged element and be combined with the exact negative value from the damaged element. In such a case, a diagonal in the global stiffness matrix is zero, thus

leading to singularity. While this possibility exists, it was not encountered in the cases tested herein.

In addition, although no numerical instabilities were encountered in the solved examples, further future numerical studies need to be undertaken to study the numerical stability in larger problems and with those with more complex piece-wise linear stress-strain curves.

5. Conclusions

A new method, CITA, for the damage analysis of concrete members was introduced. The method employs a piece-wise linear stress-strain curve and tangent elasticity modulus to calculate stiffness matrices including parts with negative values. In this research a simple, effectively one-dimensional stress-strain behaviour of concrete was used to study concrete beams under proportional loading. The only source of non-linearity considered was concrete fracture in tension.

By accepting the existence of indefinite tangent stiffness matrices, CITA can efficiently solve problems with softening behaviour such as concrete beams failing due to tension cracking. An appropriate equation solver with the ability to solve indefinite matrices was used to solve the tangent stiffness equation. As the presence of an indefinite tangent stiffness matrices is an indication of instability, an analysis control method had to be used. The method adopted in CITA to control this instability was the gradual introduction of damage. With the combination of a piece-wise linear stress-strain diagram, accepting indefinite tangent stiffness matrices, and a gradual damage introduction, the CITA method was formulated and applied to the solution of concrete beams failing due to tension cracking. The combination of these features in CITA method was demonstrated to produce an efficient and stable new method for the analysis of the highly non-linear problem of concrete beams failing by tension cracking.

Notably, the CITA method can be easily implemented into existing non-linear analysis software with minimal change. The main changes are related to the calculation of the load factor and the use of a linear equation solver that can handle indefinite stiffness matrices. Finally, the authors believe that the method can be applied to the analysis of other materials such as reinforced concrete, masonry, and glass. This will be investigated in a future research. The piece-wise linear stress-strain idealisation is a fundamental part of CITA. Other current limitations such as proportional loading and non-linear compression behaviour are not considered to be crucial limitations. These will be studied in future research. Another aspect that deserves further investigation is to study the possibility of encountering singularity during solution.

References

[1] M.A. Crisfield, Non-linear finite element analysis of solids and structures, John Wiley & Sons Ltd., Chichester (1996)

[2] P. Wriggers, Nonlinear finite element methods, Springer Science & Business Media (2008)

[3] H. Schlune, M. Plos, K. Gylltoft, Safety formats for non-linear analysis of concrete structures, Mag Concr Res, 64 (2012), pp. 563–574

[4] ANSYS, Workbench user' s guide. Release 15, Southpointe 275 Technology Drive, Canonsburg, PA 15317 (2013)

[5] Abaqus 6.1, Analysis user's manual, Dassault Systèmes Simulia Corp., Pawtucket, RI (2010)

[6] ATENA: User's manual for ATENA 3D. Prague; 2015.

[7] A.M.P. Valli, R.N. Elias, G.F. Carey, A.L.G.A. Coutinho, PID adaptive control of incremental and arclength continuation in nonlinear applications, Int J Numer Methods Fluids, 61 (2009), pp. 1181–1200

[8] M.A. Crisfield, An arc-length method including line searches and accelerations, Int J Numer Methods Eng, 19 (1983), pp. 1269–1289

[9] R. Graça-E-Costa, J. Alfaiate, D. Dias-Da-Costa, L.J. Sluys, A non-iterative approach for the modelling of quasi-brittle materials, Int J Fract, 178 (2012), pp. 281–298

[10] M.A.N. Hendriks, J.G. Rots, Sequentially linear versus nonlinear analysis of RC structures, Eng Comput, 30 (2013), pp. 792–801

[11] Rots JG. Sequentially linear continuum model for concrete fracture. In: R. de Borst, J. Mazars GP-C and JGM van M, editor. Fract. Mech. Concr. Struct. Proc. Fram., Lisse. The Netherlands: A.A. Balkema; 2001, p. 831–9.

[12] J.G. Rots, S. Invernizzi, Regularized sequentially linear saw-tooth softening model, Int J Numer Anal Methods Geomech, 28 (2004), pp. 821–856

[13] J.G. Rots, B. Belletti, S. Invernizzi, Robust modeling of RC structures with an "event-by-event" strategy, Eng Fract Mech, 75 (2008), pp. 590–614

[14] C. Louter, A.van de Graaf, J. Rots, Modeling the structural response of reinforced glass beams using an SLA scheme, Challenging Glas. 2 – Conf. Archit. Struct. Appl. Glas., TU Delft (2010)

[15] G. Giardina, Modelling of settlement induced building damage, Delft University of Technology, TU Delft (2013)

[16] A.T. Slobbe, M.A.N. Hendriks, J.G. Rots, Sequentially linear analysis of shear critical reinforced concrete beams without shear reinforcement, Finite Elem Anal Des, 50 (2012), pp. 108–124

[17] M.J. DeJong, M.A.N. Hendriks, J.G. Rots, Sequentially linear analysis of fracture under non-proportional loading, Eng Fract Mech, 75 (2008), pp. 5042–5056

[18] J. Eliáš, Generalization of load-unload and force-release sequentially linear methods, Int J Damage Mech, 24 (2015), pp. 279–293

[19] S. Invernizzi, D. Trovato, M.A.N. Hendriks, A.V. Van de Graaf, Sequentially linear modelling of local snap-back in extremely brittle structures, Eng Struct, 33 (2011), pp. 1617–1625

[20] A.T. Slobbe, Propagation and band width of smeared cracks, Delft University of Technology (2015)

[21] G.H. Golub, C.F. Van Loan, Matrix computations, (4th ed.) JHU Press, Baltimore (2012)

[22] J.R. Bunch, L. Kaufman, Some stable methods for calculating inertia and solving symmetric linear systems, Math Comput, 31 (1977), pp. 163–179
[23] J.O. Aasen, On the reduction of a symmetric matrix to tridiagonal form, BIT, 11 (1971), pp. 233–242
[24] O. Schenk, K. Gärtner, On fast factorization pivoting methods for sparse symmetric indefinite systems, Electron Trans Numer Anal, 23 (2006), pp. 158–179
[25] Misson WW, Studley CK, West WJ, Liljenwall ET. Keyboard having switches with tactile feedback. US Patent 3941953 A; 1976.
[26] A.A. Sarlis, D.T.R. Pasala, M.C. Constantinou, A.M. Reinhorn, S. Nagarajaiah, D.P. Taylor, Negative stiffness device for seismic protection of structures, J Struct Eng (2012), p. 468
[27] D. Ngo, A.C. Scordelis, Finite element analysis of reinforced concrete beams, J ACI, 64 (1967), pp. 152–163
[28] J.G. Rots, J. Blaauwendraad, Crack models for concrete, discrete or smeared?
Fixed, multi-directional or rotating?, vol. 34, Delft, The Netherlands (1989)
[29] Y.R. Rashid, Ultimate strength analysis of prestressed concrete pressure vessels, Nucl Eng Des, 7 (1968), pp. 334–344
[30] R. de Borst, J.J.C. Remmers, A. Needleman, M.A. Abellan, Discrete vs smeared crack models for concrete fracture: Bridging the gap, Int J Num Anal Methods Geomech, 28 (2004), pp. 583–607
[31] N. Moës, J. Dolbow, T. Belytschko, A finite element method for crack growth without remeshing, Int J Num Meth Eng, 46 (1999), pp. 131–150
[32] Z.P. Bazant, M. Jirásek, Nonlocal integral formulations of plasticity and damage: survey of progress, J Eng Mech, 128 (2002), pp. 1119–1149
[33] Task Committee on Finite Element Analysis of Reinforced Concrete Structures, State-of-the-art report on finite element analysis of reinforced concrete, ASCE, New York (1982)
[34] L. Jason, A. Huerta, G. Pijaudier-Cabot, S. Ghavamian, An elastic plastic damage formulation for concrete: application to elementary tests and comparison with an isotropic damage model, Comput Methods Appl Mech Eng, 195 (2006), pp. 7077–7092
[35] Z.P. Bazant, L. Cedolin, Blunt crack band propagation in finite element analysis, J Eng Mech Div, 105 (1979), pp. 297–315
[36] L. Cedolin, Z.P. Bazant, Effect of finite element choice in blunt crack band analysis, Comput Methods Appl Mech Eng, 24 (1980), pp. 305–316
[37] Z.P. Bazant, B.H. Oh, Crack band theory for fracture of concrete, Mater Struct (1983), pp. 155–177 January-February
[38] R. Graça-E-Costa, J. Alfaiate, D. Dias-Da-Costa, P. Neto, L.J. Sluys, Generalisation of non-iterative methods for the modelling of structures under non-proportional loading, Int J Fract, 182 (2013), pp. 21–38
[39] P.E. Petersson, Crack growth and development of fracture zones in plain concrete and similar materials, Lund, Sweden (1981)
[40] The International Federation for Structural Concrete, fib Model Code for Concrete Structures 2010, (1st ed.) Ernst & Sohn (2013)